Special Interest Group Meeting on Thermal Issues
Laboratory for Machine Tools and Production Engineering (WZL) of
RWTH Aachen, Germany, February 2020
www.euspen.eu

Input-Output Linearized Control of a Thermoelectric Actuator using an Extended Kalman Filter Observer

Koen Bos[1], Dennis Heck[2], Robert van der Kall[2], and Marcel Heertjes[3]

[1]*ASML, Development & Engineering, Thermal Architecture EUV Scanner*
[2]*ASML, Development & Engineering, Thermal Architecture DUV Scanner*
[3]*Eindhoven University of Technology, Mechanical Engineering, Dynamics & Control*

Corresponding author: koen.bos@asml.com

Abstract
In ASML's wafer scanners, thermal management is becoming increasingly important as a result of Moore's law driving the performance and throughput requirements. To this end, thermoelectric modules (TEMs) or Peltier elements are increasingly considered in active control of the temperature of several wafer scanner modules. TEMs are thermal actuators that have the appealing property that they are able to both cool and heat. As a disadvantage, the thermal dynamics of a TEM are nonlinear, which complicates the control design for thermoelectric systems. Due to the inherent nonlinearity, the input-output response varies significantly for different setpoints and operating conditions. This complicates the controller tuning for desired performance and compromises closed-loop stability properties for, e.g., unreachable setpoints or (unknown) disturbances, possibly causing machine downtime and damage. To deal with these problems, an input-output linearizing controller in conjunction with a linear (e.g. PID) controller is used. More specifically, to eliminate the need for temperature sensors, that might limit the thermal efficiency and performance of the actuator, we propose to use an observer to estimate the temperatures required for the IO linearization.

Thermal Control, Thermoelectric modules, Nonlinear control, Feedback Linearization, Observer

1. Introduction

In advanced lithography systems that are used to manufacture integrated circuits (ICs) (see Figure 1), thermal management in terms of accurate temperature control becomes increasingly important. For next-generation thermal conditioning, active methods using thermoelectric modules (TEMs) are receiving increased attention. TEMs are solid-state thermal actuators that use the Peltier effect to transfer heat. These actuators are broadly applied in temperature control applications, e.g. lab-on-a-chip applications, laser diodes, and scanning electron microscopes [1, 2]. Unfortunately, the thermal dynamics of TEMs are highly nonlinear [2], which complicates control design for these actuators.

To address this problem, several approaches have been studied in literature. In [1], an input-output (IO) linearizing controller is proposed, which is able to deliver fast and accurate closed-loop control of a thermoelectric system. However, stability of this controller is not guaranteed *a priori*. In another approach, a nonlinear Lyapunov-based controller is used to control a thermoelectric system with guaranteed stability [3]. However, closed-loop performance in terms of settling time, rise time, and overshoot may be difficult to guarantee, because of the nonlinear nature of the controller.

To deal with these problems, Bos *et al.* propose to use an input-output (IO) linearizing controller in conjunction with a Lyapunov-based saturation function in a generic control application of a TEM [4]. This control architecture enables linear closed-loop behaviour with a well-defined performance for nominal operating conditions, and guarantees input-to-state stability (ISS) outside these nominal operating conditions. This approach requires state knowledge pertaining to the temperatures of both sides of the TEM. Temperature sensors are placed directly on the TEM, but this introduces an additional thermal resistance between the TEM and the conditioned object on one side and the cooling water on the other side. This additional thermal resistance limits the achievable energy efficiency, and hence, the achievable performance of the TEM.

To overcome this problem, we propose to use an extended Kalman filter (EKF) to estimate the required states for the IO linearization. This eliminates the need for sensors placed directly on the TEM. As such, the first key contribution is the design of the EKF for a nonlinear thermoelectric system. The second contribution is the implementation and verification of the results on an experimental setup.

The remainder of this abstract is organized as follows. Section 2 introduces the system at hand and summarizes the control architecture proposed in [4], as it forms the basis for this work. Section 3 presents the observer design for the thermoelectric system. Section 4 shows experimental results obtained from an experimental setup. Finally, Section 5 presents concluding remarks and recommendations for further research.

Figure 1. ASML's EUV System

2. System Description

In accordance with [4], an experimental setup is considered that resembles a simplified thermal control application in a wafer scanner, as illustrated in Figure 2 and Figure 3.

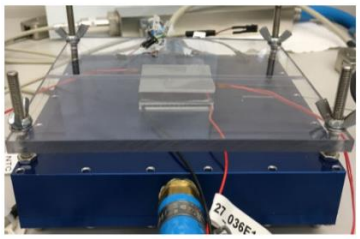

Figure 2. Experimental thermoelectric setup [4].

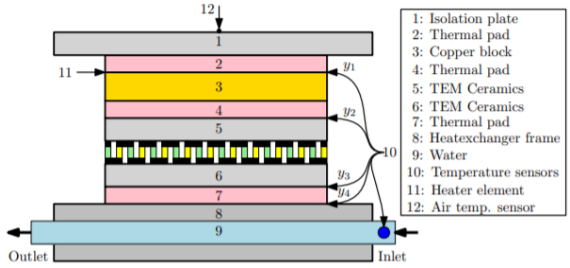

Figure 3. Schematic of the experimental thermoelectric setup [4].

2.1. Experimental Setup

The setup consists of a copper block (element 3 in Figure 3) attached to a thin film heater (element 11) that resembles a heat dissipating module, a thermoelectric module (type UWE UEPT-140-127-036E120) (element 5,6) used as a thermal actuator to condition the copper block, a heat exchanger (element 8) connected to a cooling water circuit (element 9) to remove waste-heat from the system. These components are assembled using thermal pads (element 2,4,7). The top plate (element 1) is used for assembly purposes. In the setup, four negative temperature coefficient (NTC) sensors are located between components of the setup (y_1 to y_4 in Figure 3), and two NTC sensors are used to measure the inlet water temperature of the heat exchanger and the surrounding air temperature, respectively.

2.2. Thermal Dynamics & IO linearization

The setup is modelled using a lumped mass approach, resulting in the following set of ordinary differential equations (ODEs):

$$\begin{aligned}
E_1\dot{x}_1 &= \frac{1}{R_{12}}(x_2 - x_1) + \frac{1}{R_\infty}(w_2 - x_1)\\
E_2\dot{x}_2 &= \frac{1}{R_{12}}(x_1 - x_2) + \frac{1}{R_{23}}(x_3 - x_2)\\
E_3\dot{x}_3 &= \frac{1}{R_{23}}(x_2 - x_3) + \frac{1}{R_{34}}(x_4 - x_3) + w_3\\
E_4\dot{x}_4 &= \frac{1}{R_{34}}(x_3 - x_4) + \frac{1}{R_{45}}(x_5 - x_4)\\
E_5\dot{x}_5 &= \frac{1}{R_{45}}(x_4 - x_5) + \frac{1}{R_{56}}(x_6 - x_5) + u^2R_e/2 - Sx_5u\\
E_6\dot{x}_6 &= \frac{1}{R_{56}}(x_5 - x_6) + \frac{1}{R_{67}}(x_7 - x_6) + u^2R_e/2 + Sx_6u\\
E_7\dot{x}_7 &= \frac{1}{R_{67}}(x_6 - x_7) + \frac{1}{R_{78}}(x_8 - x_7)\\
E_8\dot{x}_8 &= \frac{1}{R_{78}}(x_7 - x_8) + \frac{1}{R_{89}}(x_9 - x_8)\\
E_9\dot{x}_9 &= \dot{m}c_w(w_1 - x_9) + \frac{1}{R_{89}}(x_8 - x_9),
\end{aligned} \tag{1}$$

with $x_i, i \in \{1,2,\dots,9\}$ representing the temperatures of the lumped elements in Figure 3, E_i the thermal capacitance of the elements, $R_{i,i+1}$ the thermal resistances between elements, R_∞ the thermal resistance between the surrounding air and the top plate. These parameters are calibrated using a dedicated experiment, see [4] for the details. Furthermore, w_1 is the temperature of the water at the inlet of the heat exchanger, w_2 the surrounding air temperature, w_3 the thermal power of the thin film heater (representing thermal disturbance loads), $\dot{m}$ the mass flow of the water, and c_w the specific heat capacity of the water. Finally, S represents the Seebeck coefficient, u the applied electric current, and R_e the electrical resistance of the TEM. The control output y is the temperature of the copper block measured by the sensor y_1 (see Figure 3), and is defined as

$$y = y_1 = \alpha_1 x_2 + (1 - \alpha_1)x_3, \tag{2}$$

with α_1 a scaling factor to account for the fact that the sensor is located in between element 2 and 3.

In (1) the (input) nonlinearity is clearly visible in the terms containing u^2 and x_5u and x_6u, that relate to the Joule heating effect and Peltier and Seebeck effect of the TEM [2, 4]. To overcome the nonlinearity between the input u and the output y, the IO linearization as proposed in [4] is considered with a newly defined input:

$$v = \frac{1}{R_{56}}(x_6 - x_5) - Sx_5u + u^2R_e/2. \tag{3}$$

After substitution of the new input v of (3) in (1), the IO dynamics of the system can be written as

$$\begin{aligned}
E_1\dot{x}_1 &= \frac{1}{R_{12}}(x_2 - x_1) + \frac{1}{R_\infty}(w_2 - x_1)\\
E_2\dot{x}_2 &= \frac{1}{R_{12}}(x_1 - x_2) + \frac{1}{R_{23}}(x_3 - x_2)\\
E_3\dot{x}_3 &= \frac{1}{R_{23}}(x_2 - x_3) + \frac{1}{R_{34}}(x_4 - x_3) + w_3\\
E_4\dot{x}_4 &= \frac{1}{R_{34}}(x_3 - x_4) + \frac{1}{R_{45}}(x_5 - x_4)\\
E_5\dot{x}_5 &= \frac{1}{R_{45}}(x_4 - x_5) + v.
\end{aligned} \tag{4}$$

The remaining nonlinear zero-dynamics are then constituted by

$$\begin{aligned}
E_6\dot{x}_6 &= \frac{1}{R_{56}}(x_5 - x_6) + \frac{1}{R_{67}}(x_7 - x_6) + u^2R_e/2 + Sx_6u\\
E_7\dot{x}_7 &= \frac{1}{R_{67}}(x_6 - x_7) + \frac{1}{R_{78}}(x_8 - x_7)\\
E_8\dot{x}_8 &= \frac{1}{R_{78}}(x_7 - x_8) + \frac{1}{R_{89}}(x_9 - x_8)\\
E_9\dot{x}_9 &= \dot{m}c_w(w_1 - x_9) + \frac{1}{R_{89}}(x_8 - x_9),
\end{aligned} \tag{5}$$

with u the linearizing control law (following from (3)) as

$$u = \frac{Sx_5 - \sqrt{S^2x_5^2 - 2R_e(\frac{1}{R_{56}}(x_6 - x_5) - v}}{R_e}. \tag{6}$$

This control poses a lower-limit on the allowed input v, as to guarantee that the input u remains real-valued, or

$$v \geq \frac{1}{R_{56}}(x_6 - x_5) - \frac{S^2x_5^2}{2R_e}. \tag{7}$$

Physically, this lower bound is the maximum possible cooling power the TEM, that depends on the temperatures of the cold and hot-side of the TEM (x_5 and x_6, respectively). For this reason, it is important to ensure input-to-state stability of the nonlinear differential equations in (5), as to prevent the state x_6 from becoming too large and consequently limiting the cooling power of the TEM through (7).

2.3. Control Architecture

In [4], the linearizing control law (6), is implemented in a control loop in combination with a saturation function Φ and linear feedback controller C_{fb}, as shown schematically in Figure 4. The saturation function ensures that the computed control

input by the feedback controller $\bar{v}$ stays within predetermined Lyapunov-based bounds, or

$$\Phi: \quad v = min\{max\{\bar{v}, \beta_2\}, \beta_3\}, \tag{8}$$

with β_2 and β_3 bounds derived from a Lyapunov stability analysis. This effectively guarantees input-to-state stability of the closed-loop system, while allowing for linear closed-loop IO behaviour in normal operating conditions.

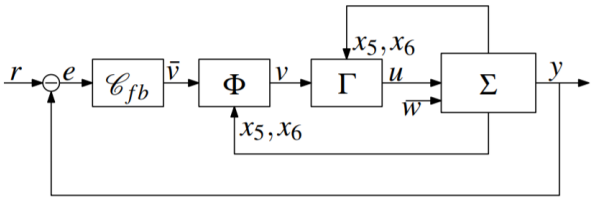

Figure 4. Schematics of the IO linearizing controller architecture [4].

3. Observer

As shown in Figure 4, the IO linearizing controller Γ and the saturation function Φ require state knowledge of x_5 and x_6 (the TEM temperatures). In [4], sensors are used to measure these states, but this sensor placement negatively affects the contact resistance and thus the thermal performance.

As a solution to this problem, an observer will be used to estimate the required states, using only sensors y_1 and y_4 that are not attached to the TEM, but are usually already available for diagnostics and feedback control. Furthermore, we consider the known inputs of the system to be the electric current u, inlet water temperature w_1 and air temperature w_2. The heat load of the heater is considered as an unknown disturbance w_3.

With this, system (1) is written in state-space formulation according to

$$\Sigma: \begin{cases} \dot{x} = F(x, u, w) \\ y = Cx + \eta \end{cases} \tag{9}$$

with $y = [y_1 \quad y_4]^T$ the measurements of the connected sensors, $w = [w_1 \quad w_2 \quad w_3]^T$ the disturbances acting on the system and η representing measurement noise. Note that $F(x, u, w)$ represents the equations in (1).

3.1. Extended Kalman Filter

The extended Kalman filter (EKF), which is commonly used in nonlinear state estimation, is known to deliver accurate results for temperature estimation [5]. The continuous-time EKF for the system (9) reads

$$\hat{\Sigma}: \begin{cases} \dot{\hat{x}} = F(\hat{x}, u, \hat{w}) - K(t)(C(x - \hat{x}) + \eta) \\ K(t) = P(t)C^T R^{-1} \\ \dot{P} = A(t)P + PA^T(t) - PC^T R^{-1} CP + Q, \end{cases} \tag{10}$$

with $\hat{x}$ the state estimate, $\hat{w} = [w_1 \; w_2 \; 0]^T$ the measured (known) disturbances, $K(t)$ the time-varying Kalman gain, $P(t)$ the estimated error covariance, Q and R tuning matrices, and $A(t)$ a linearization of the process $F(\hat{x}, u, \hat{w})$, which is defined as

$$A(t) = A(u(t)) = \frac{\partial F(x, u, w)}{\partial x} = \frac{\partial F(\hat{x}, u, w)}{\partial \hat{x}}. \tag{11}$$

Note that the resulting matrix $A(t)$ only depends on $u(t)$ and does not depend on x nor $\hat{x}$. Therefore, the linearization of F around $\hat{x}$ is equal to the linearization of F around x, as stated in (10). Exploiting the latter, stability of the EKF itself can be shown by means of Lyapunov theory. To this end, consider the Lyapunov function candidate

$$V = \epsilon^T P(t)^{-1} \epsilon, \tag{12}$$

with $\epsilon = x - \hat{x}$ the estimation error and $P(t)^{-1}$ the inverse of the error covariance matrix. The time-derivative of this Lyapunov function can be expressed as

$$\dot{V} \leq -\epsilon^T (P^{-1} Q P^{-1} + C^T R^{-1} C)\epsilon + 2\epsilon^T P^{-1} B_d (w - \hat{w}) + 2\epsilon^T P^{-1} P C^T R^{-1} \eta \tag{13}$$

with $B_d = \partial F / \partial w$. By using the fact that $\dot{P}^{-1} = -P^{-1}\dot{P}P^{-1}$ and $C^T R^{-1} C \geq 0$, and substituting (12) into (13):

$$\begin{aligned} \dot{V} &\leq -\frac{q}{\bar{p}^2}\|\epsilon\|^2 + \frac{2}{E_3 \underline{p}}\|\epsilon\|\|w_3\| + \frac{2\bar{c}}{\underline{r}}\|\epsilon\|\|\eta\| \\ &\leq -\frac{qp}{\bar{p}^2} V + \frac{2}{E_3 \underline{p}}\sqrt{\bar{p}V}\|w_3\| + \frac{2\bar{c}}{\underline{r}}\sqrt{\bar{p}V}\|\eta\|, \end{aligned} \tag{14}$$

with $\underline{q}, \underline{p}, \underline{r}$ (norm-based) lower bounds on the matrices Q, P and R, and $\bar{p}, \bar{c}$ (norm-based) upper bounds on the matrices P and C, respectively. Using a new function $W = \sqrt{V}$, analogous to [6], the following bound on the estimation error can be derived from (14):

$$\begin{aligned} \|\epsilon(t)\| \leq \sqrt{\frac{\bar{p}}{\underline{p}}}\|\epsilon(0)\| e^{-\theta t} &+ \frac{\bar{p}}{\theta E_3 \underline{p}}\left(1 - e^{-\theta t}\right) \sup_{t \geq t_0} w_3(t) \\ &+ \frac{\bar{c}\bar{p}}{\theta \underline{r} \underline{p}}\left(1 - e^{-\theta t}\right) \sup_{t \geq t_0} \eta(t), \end{aligned} \tag{15}$$

with $\theta = \underline{qp}/2\bar{p}^2$. With this bound, the EKF is concluded to be input-to-state stable in the presence of the unknown disturbance $w_3(t)$ and measurement noise $\eta(t)$.

3.2. Implementation

The EKF in (10) is used in closed-loop with the control architecture from [4], as illustrated in Figure 5. The estimated states $\hat{x}$ that are computed by the EKF, are used as inputs to the IO linearizing controller Γ and the saturation function Φ. In linear systems, the separation principle guarantees stability for a closed-loop system with a separately designed stable observer and controller. However, for nonlinear systems, the separation principle often does not hold [7], meaning that stability cannot be automatically concluded when using a stable EKF for closed-loop control. In [8], a separation principle for a class of nonlinear systems is presented. However, the method used in [8] requires that the control law is continuously differentiable, which is in this case not applicable because of the saturation function Φ. In [9], an analysis is conducted on closed-loop stability of a system under EKF-based feedback, however, the analysis used is limited to systems that can be written in a special normal form, which is found not possible in this case. In the remainder of this work, closed-loop stability is assumed and verified experimentally in the next section.

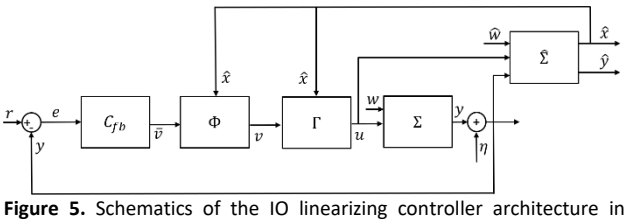

Figure 5. Schematics of the IO linearizing controller architecture in conjunction with the extend Kalman filter.

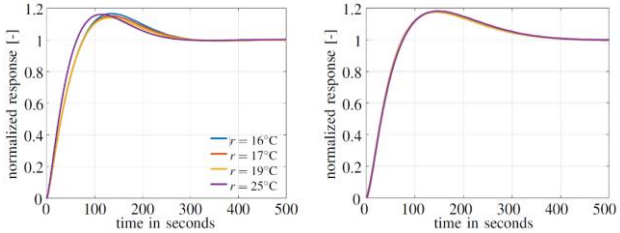

Figure 6. Measured (normalized) closed-loop step responses with a PID controller (left) [4], and the responses with IO linearization and EKF (right).

4. Measurement Results

To verify the obtained results in this work, an experiment is conducted by varying the setpoint temperature and using the estimated state by the EKF in the IO linearization. Analogous to [4], Figure 6 depicts the *normalized* step response without (left) and with (right) IO linearization. From this figure, it is observed that the estimation error of the EKF has little impact on the linearization of the IO dynamics, because all responses in the right plot are identical.

To verify the closed-loop stability of the system as a whole, a second experiment is conducted by applying a heat-load of $w_3(t)$ =12W with the heater, and commanding an unreachable setpoint of $r = -20$ °C, similar to the experiment conducted in [4]. This experiment does not come with any stability guarantees, but the closed-loop system is still found to be stable, as shown in Figure 7. In the left part of Figure 7, the outputs y_1 and y_4 are shown. The output y_1 is controlled toward the setpoint $r = -20$ °C, but this temperature cannot be reached, because of the applied heat-load and the limitations of the TEM. As also shown in [4], this situation would lead to instability if only a PID controller would be used. However, the stability bound β_2 limits the input $\bar{v}$ (as computed by the linear controller C_{fb}) and applies a limited input v to ensure stability, as shown in the right part of Figure 7.

By comparing this result to the results depicted in Figure 8 as obtained from [4], it can be concluded that the performance with the EKF exceeds the performance (in terms of reachable temperature y_1) of using sensors to estimate the required state variables x_5 and x_6. It is worth noting that, although not used, the sensors y_2 and y_3 are still physically present in the setup, in order to make a fair comparison to the results obtained in [4].

It is assumed that the difference in performance is due to the location of the sensors (in between elements) and that they therefore do not exactly measure the states they are assumed to represent. This, in turn, would lead to a larger error than the error of the state estimation by the EKF. This larger error caused by the sensor placement leads to a more conservative bound β_2, such that less cooling power is available when compared to using the EKF. This can partly be explained by the performed calibration of model parameters in [4], where an accurate match is obtained between measurements and model simulations. The model-based EKF naturally benefits from this calibration of parameters.

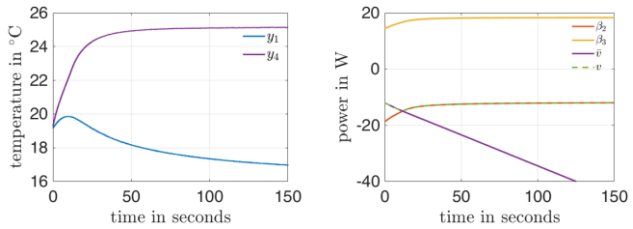

Figure 7. Measured output (left) and input bounds (right) of the experiment with the EKF and the nonlinear controller obeying the bounds $\beta_2(\hat{x}_5, \hat{x}_6), \beta_3(\hat{x}_5, \hat{x}_6)$.

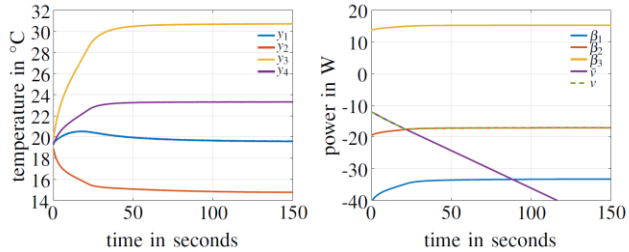

Figure 8. Measured output (left) and input bounds (right) of the experiment without EKF [4] .

5. Conclusions and Recommendations

For a thermoelectric system, this paper demonstrates the successful design and implementation of an extended Kalman filter with the IO linearizing control architecture proposed in [4]. The observer eliminates the need for sensors to be attached to the TEM, which otherwise limits performance. The estimated states can directly be used in the IO linearizing controller and saturation function. In the conducted experiment, the achieved performance supersedes the performance obtained in [4], in which sensors are used instead of an observer. This performance increase is attributed to the accuracy of the state-estimation by the EKF, because the unused sensors (that are attached to the TEM) are still physically present in the setup, meaning the thermal contact resistances are equal in both experiments. It is concluded that the accurate state-estimation allows for a less conservative stability bound with respect to the situation where sensors are used to estimate the required temperatures. Furthermore, no stability issues pertaining to using an observer in closed-loop were observed.

For future work, our research focusses on applying the control architectures with and without EKF to a system with multiple thermoelectric actuators. Furthermore, we will focus on obtaining stability guarantees for using the observer in the loop. Finally, we will investigate the sensitivity of the EKF to uncertainty in the model parameters.

References

[1] R. van Gils, "Practical thermal control by thermo-electric actuators," *2017 23rd Int. Workshop on Thermal Investigations of ICs and Systems (THERMINIC*), Amsterdam, 2017, pp. 1-6.

[2] J. Jiang, G. Kaigala, H. Marquez, and C. Blackhouse, Nonlinear Controller Designs for Thermal Management in PCR Amplification, *IEEE Tr. on Control Systems Technology*, 20(1), pp. 11-30, 2012.

[3] A. Mironova, P. Mercorelli, A. Zedler, Robust Control using Sliding Mode Approach for Ice-Clamping Device activated by Thermoelectric Coolers, *In IFAC-PapersOnLine, 49(25),* pp. 470-475, 2016.

[4] K. Bos, D. Heck, M. Heertjes and R. van der Kall, "IO Linearization, Stability, and Control of an Input Non-Affine Thermoelectric System," *2018 Annual American Control Conference (ACC),* Milwaukee, WI, 2018, pp. 526-531.

[5] A. Yanou, N. Hosoya, K. Wada, M. Minami, and T. Matsuno, “Estimation of thermal conductivity for model with radiative heat transfer by extended Kalman filter,” in 2016 IEEE 21st Int. Conf. on Emerging Technologies and Factory Automation (ETFA), pp. 1–4, Sept 2016.

[6] H. Khalil, *Nonlinear Systems, ch. 5*, pp. 223–225. Edinburgh Gate, Harlow: Pearson, second ed., 1996.

[7] A. Fossard and D. Normand-Cyrot, *Nonlinear Systems: Modeling and Estimation, ch. 5*, pp. 173–213. Nonlinear Systems, Springer US, 1995.

[8] A. E. Golubev, A. P. Krishchenko, and S. B. Tkachev, “Separation principle for a class of nonlinear systems,” *IFAC Proc. Volumes, vol. 35*, no. 1, pp. 447 – 452, 2002. 15th IFAC World Congress.

[9] J. H. Ahrens and H. K. Khalil, “Closed-loop behaviour of a class of nonlinear systems under EKF-based control,” *IEEE Tr. on Automatic Control, vol. 52*, pp. 536–540, March 2007.